

# Fast processing techniques for accurate ultrasonic range measurements

To cite this article: Billur Barshan 2000 *Meas. Sci. Technol.* **11** 45

View the [article online](#) for updates and enhancements.

## Related content

- [Advanced Digital Imaging Laboratory Using MATLAB® : Image correlators for detection and localization of objects](#)  
L P Yaroslavsky
- [Multiple ultrasonic range measurements](#)  
Billur Barshan, Deniz Baskent and Billur Barshan
- [Performance analysis of ultrasonic ranging using a digital polarity correlator](#)  
T Kodama and K Nakahira

## Recent citations

- [Tugba Ozge Onur and Rifat Hacıoğlu](#)
- [Correction of cosine oscillation to the improved correlation method of estimating the amplitude of gravitational background signal](#)  
Wei-Huang Wu *et al*
- [An improved correlation method for amplitude estimation of gravitational background signal with time-varying frequency](#)  
Wei-Huang Wu *et al*

# Fast processing techniques for accurate ultrasonic range measurements

Billur Barshan

Department of Electrical Engineering, Bilkent University, 06533 Bilkent, Ankara, Turkey

E-mail: billur@ee.bilkent.edu.tr

Received 2 August 1999, in final form and accepted for publication 3 November 1999

**Abstract.** Four methods of range measurement for airborne ultrasonic systems—namely simple thresholding, curve-fitting, sliding-window, and correlation detection—are compared on the basis of bias error, standard deviation, total error, robustness to noise, and the difficulty/complexity of implementation. Whereas correlation detection is theoretically optimal, the other three methods can offer acceptable performance at much lower cost. Performances of all methods have been investigated as a function of target range, azimuth, and signal-to-noise ratio. Curve fitting, sliding window, and thresholding follow correlation detection in the order of decreasing complexity. Apart from correlation detection, minimum bias and total error is most consistently obtained with the curve-fitting method. On the other hand, the sliding-window method is always better than the thresholding and curve-fitting methods in terms of minimizing the standard deviation. The experimental results are in close agreement with the corresponding simulation results. Overall, the three simple and fast processing methods provide a variety of attractive compromises between measurement accuracy and system complexity. Although this paper concentrates on ultrasonic range measurement in air, the techniques described may also find application in underwater acoustics.

**Keywords:** range measurement, time-of-flight measurement, ultrasonics, sonar, thresholding, sliding window, correlation detection, target localization and identification

## 1. Introduction

Successful operation of most ultrasonic ranging systems relies on accurate *time-of-flight* (TOF) measurements. A pulse is transmitted and an echo is produced when the transmitted pulse encounters an object. TOF is the time elapsed between the transmission of a pulse and its reception, from which the target range can be calculated as  $r = ct_0/2$ . Here,  $t_0$  is the TOF and  $c$  is the speed of sound in air†. Range information forms the basis of many applications such as object localization, classification, and tracking [1–3]. Correct localization of targets using ultrasonics depends on how accurately TOF can be measured and how well the speed of sound in the medium is known. The dependence of sound velocity on temperature can be relatively easily compensated for [4]. Since we employ a pulse–echo system, the measurements are not significantly affected by movements of the propagation medium. The most frequently employed method for TOF measurement is, due to its simplicity, *thresholding*. In simple thresholding systems, a range value  $r$  is produced when the echo amplitude first

exceeds a preset threshold level. The main problem with this method is that, on the average, the TOF measurement so obtained is larger than the actual TOF, which corresponds to the starting point (onset) of the echo signal. This is a consequence of the relatively long rise-time of the echoes produced by currently available low-bandwidth ultrasonic transducers for operation in air. Hence, the range information obtained by simple thresholding is biased, making the target appear slightly farther than it actually is. The resulting bias error, which is in the range of several millimetres to centimetres, could easily be avoided if it were constant. However, this is not the case: the bias is difficult to model analytically since it is a function of the set threshold level, signal-to-noise ratio (SNR), target location, size, and type, as well as other factors [5] causing amplitude fluctuations. In this paper, we consider two alternative fast methods, namely curve fitting and sliding window, which reduce the bias and improve robustness to noise.

All of the three methods mentioned so far are suboptimal but fast and simple to implement in real time. These methods are compared with the optimal *correlation detection method* which maximizes the SNR. In this study, the SNR is taken as the ratio of the maximum amplitude of the echo signal to the amplitude noise standard deviation. Comparison of

†  $c \cong 331.4\sqrt{T/273} \text{ m s}^{-1}$ , where  $T$  is the absolute temperature in Kelvin. At room temperature,  $c = 343.5 \text{ m s}^{-1}$ . This expression neglects effects such as those due to humidity and pressure.

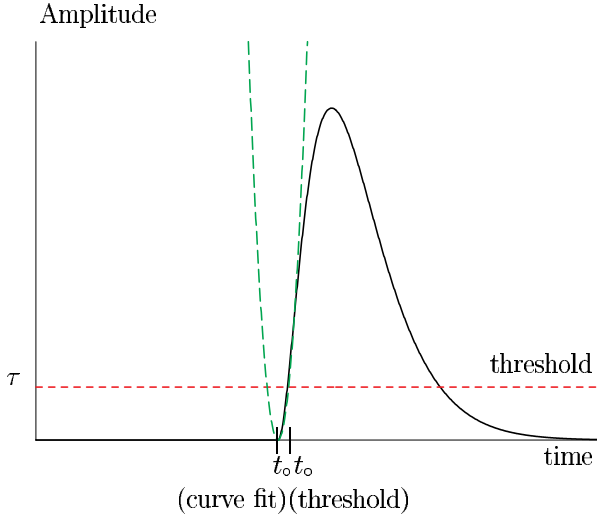


**Figure 1.** Envelope of the ultrasonic echo and TOF measurement by thresholding and curve fitting.

the methods is based on bias, standard deviation, total error, robustness to noise, and computational complexity.

This paper has been divided into four sections, the first being the introduction. Section 2 gives a brief description of the four TOF measurement methods considered in this paper. Sections 3 and 4 provide the simulation and experimental results, respectively.

## 2. TOF measurement and estimation

### 2.1. Thresholding method

The simplest way of measuring TOF is thresholding. In the *thresholding* method, the TOF is the time  $t_0$  at which the echo amplitude waveform first exceeds a preset threshold level  $\tau$  (figure 1). Assuming Gaussian noise,  $\tau$  is usually set equal to 3–5 times the noise standard deviation. In current practical ultrasonic systems, with this choice, the threshold level turns out to be between  $-20$  to  $-35$  dB below the peak of the pulse.

### 2.2. Curve-fitting method

Another TOF estimation method is *curve fitting*, in which a nonlinear least-squares method is employed to fit a curve to the onset of the ultrasonic echo in order to produce an unbiased TOF measurement. A parabolic curve of the form  $a_0(t - t_0)^2$  is fitted to the signal envelope around the rising edge of the echo. It has been verified in [6, 7] and later on in [8] that this is a good approximation. First, initial estimates of the two parameters  $a_0$  and  $t_0$  are obtained: the initial estimate for  $t_0$  is found by simple thresholding, and  $a_0$  is estimated from the second derivative approximation around the threshold point. These are used to initialize an iterative numerical procedure: the Levenberg–Marquardt nonlinear least-squares method [9]. In the simulations and the experiments, 50 samples of the echo signal, taken around the threshold point, have been used to estimate the parameters  $a_0$  and  $t_0$  of the best-fitting curve. The value of  $t_0$  finally obtained, which corresponds to the vertex of the parabola, is taken as the TOF (figure 1). This value usually falls to

the left of the thresholding estimate, and reduces the bias considerably.

The authors of [8] have pointed out a simpler variation of the curve-fitting method which does not require the nonlinear iterative fitting procedure. In this method, two different threshold levels are set, and a parabola is fit to the two samples of the signal at which the threshold levels are exceeded. Let  $\tau_1$  and  $\tau_2$  be the two threshold levels ( $\tau_2 > \tau_1$ ) and  $t_1$  and  $t_2$  be the times at which these thresholds are exceeded. The parameters  $a_0$  and  $t_0$  of the parabola  $a_0(t - t_0)^2$  passing through these points can be solved from the following two equations:

$$\begin{aligned}\tau_1 &= a_0(t_1 - t_0)^2 \\ \tau_2 &= a_0(t_2 - t_0)^2.\end{aligned}\tag{1}$$

Eliminating  $a_0$  we obtain the following expression for the TOF  $t_0$ :

$$t_0 = \frac{\sqrt{\tau_2/\tau_1} t_1 - t_2}{\sqrt{\tau_2/\tau_1} - 1}.\tag{2}$$

It has been reported in [8] that a threshold ratio  $\tau_2/\tau_1$  of about 2 represents a suitable choice. In the following, to distinguish the two approaches, we will refer to the original iterative least-squares curve-fitting method as CUF(A) and the 2-point analytical curve-fitting method as CUF(B).

### 2.3. Sliding-window method

The third method considered in this study is the *sliding window*, whose use for ultrasonic signals was first suggested in [10]. The method originates from the *m-out-of-N* (or double thresholding) detection originally developed for radar signals, and is used to make detection more robust to noise [11]. A window of width  $N$  is slid through the echo signal one sample at a time. At each window position, the number of samples which exceed the preset threshold level  $\tau$  is counted. If this number exceeds a second threshold  $m$ , then a target is assumed to be present and a TOF estimate is produced. The advantage of the method is its robustness to noise spikes, since the target detection is based on at least  $m$  samples exceeding the threshold, instead of a single one as in simple thresholding. This way, noise spikes of total duration less than  $m$  can be eliminated. We have considered four different ways of choosing the TOF within the window. These are, SW(A): the very first sample of the current window, SW(B): the first sample exceeding  $\tau$  within the window, SW(C): the sample at the centre of the window, and SW(D): the  $(N - m)$ th sample of the window. The performance of the method depends on the window length  $N$ , the second threshold value  $m$ , and which variation of the method is used.

### 2.4. Optimum correlation detection

The *optimum correlation detection* method for estimating TOF from the echo signal is unbiased. Matched filter techniques have been widely used to improve the accuracy of TOF measurements in applications such as target localization and identification [1, 12, 13].

A matched filter that contains a replica of the echo waveform is employed to determine the most probable location of the echo in the received signal [14]. The computer

implementation of this procedure is time consuming because of the required correlation operation, even when realized in the frequency domain. Since the shape of the echo waveform usually changes during propagation due to attenuation, and also varies with target type, size, location, and orientation, a large number of templates for the expected signal must be stored for the correlation operation. Another fundamental problem with this method is the inherent time delay involved since classical correlation detection requires that the *entire* echo be observed before an estimate is produced. Hence, when working in real time, this method is only suitable for distant objects when the echo duration is negligible compared with the travel time. For nearby targets, or in those applications where only the leading edge of the signal is available [15] as, for instance, when the signal levels are saturated, the estimate must be made at the beginning of the observed echo, using methods such as those described above. Nevertheless, this method serves as a useful basis for comparison with the other methods.

### 3. Simulation studies

For a target at range  $r$  and azimuth  $\theta$  in the far zone of the transducer [16], the received time signal can be approximated by the following signal model [7]:

$$s_{r,\theta}(t) = k(r) \exp\left[-\frac{\theta^2}{2\sigma_\theta^2}\right] (t - t_0)^2 \exp[-a_1(t - t_0)] \times \sin[2\pi f_0(t - t_0)]u(t - t_0) \quad (3)$$

which is simply a sinusoid with frequency  $f_0$ , enveloped by a function which is the product of a parabola and an exponentially decaying function. Here,  $f_0$  is the resonance frequency of the ultrasonic transducers,  $k(r)$  is a function of the target type and is a decreasing function of the target range [6],  $a_1$  is a shape parameter of the signal, and  $u(t - t_0)$  is the unit step function delayed by  $t_0$ . The angular beam profile is modelled as a Gaussian function with suitably chosen spread  $\sigma_\theta$  [17]. The functional form of equation (3) is capable of representing observed signals for a wide variety of target types and locations [6, 7].

First, we consider the problem of finding suitable values for the window length  $N$  and the second threshold value  $m$  in the sliding-window method. Different  $N$  and  $m$  values in the range  $5 \leq N \leq 50$  and  $1 \leq m \leq N$  have been investigated for a wide range of  $r$  and  $\theta$  values. We have observed that  $N = 40$  and  $m = 10$  are suitable choices for the range of parameters considered. Thus, these values of  $N$  and  $m$  are used for the sliding-window method throughout this study. The first threshold value  $\tau$  is taken as five times the noise standard deviation in all the suboptimal methods.

In the simulations, the values  $f_0 = 40$  kHz,  $c = 343.5$  m s<sup>-1</sup>,  $\sigma_\theta = 27^\circ$ , and  $a_1 = 7050$  are used to model the echo signals obtained with Panasonic transducers. For our application of range measurement over moderate distances, the resonance frequency of available transducers lies around the range of 30–60 kHz so that the value of  $f_0$  employed can be considered to be representative. A sampling interval of  $2 \mu$ s is used, corresponding to a sampling frequency of 500 kHz. The signals are already well oversampled so that further increases would offer diminishing returns. 5000 time

samples around the echo signal are employed, corresponding to an observation window of duration 0.01 s. The value of  $r$  has been varied from 0.25 to 5.0 m with 0.25 m increments, and the value of  $\theta$  has been varied from 0 to  $55^\circ$  with  $5^\circ$  increments.

To estimate the bias and the standard deviation, 100 realizations are generated by adding zero-mean white Gaussian noise to the signal. The Gaussian noise is generated by applying a standard transformation to the uniformly distributed random variables of the C programming language. The mean and the histogram of the noise sequence are tested for bias. A comparison among the four methods and their variations is made in table 1 and figure 2 in terms of their biases, standard deviations, and total errors. We have considered the three options of processing the original time signal modelled by equation (3) (O), the rectified signal (R), and its envelope (E). The total error is the root-mean-square value of the difference between the range measurement and the actual range value. The bias is the signed average of the same difference. The three quantities are related according to  $\mathcal{E}^2 = b^2 + \sigma^2$ , where  $\mathcal{E}$  is the total error,  $b$  is the bias, and  $\sigma$  is the standard deviation.

Figures 2(a)–(f) show the dependence of the bias, the standard deviation, and the total error on  $r$  and  $\theta$ . The data for all combinations of  $r$  and  $\theta$  are not presented due to space limitations; parts (a)–(c) are for  $\theta = 0^\circ$  and parts (d)–(f) are for  $r = 0.5$  m. From the figures, we observe that the effect of increasing  $r$  and  $|\theta|$  is to degrade the range measurement accuracy. Since the noise level is kept constant, this degradation is mostly caused by the decreasing SNR due to the decrease in signal amplitude with increasing  $r$  and  $|\theta|$  (equation (3)). For example, when the target at  $r = 0.5$  m is moved from  $\theta = 0^\circ$  to  $\theta = 55^\circ$ , SNR changes from 35 to 17 dB. Similarly, when the target is moved from  $r = 0.25$  m to  $r = 5$  m along the line of sight ( $\theta = 0^\circ$ ), SNR changes from 41 to 15 dB. It can be observed that the absolute bias and the total error associated with CUF(A) increases much more slowly with  $r$  and  $|\theta|$  compared with the other methods. This quality of CUF(A) makes it attractive compared with the other methods which exhibit very large bias and total error for certain values of  $r$  and  $\theta$ .

Figures 2(g)–(i) illustrate the dependence of the performance directly on the SNR while the target position is kept constant at  $r = 0.5$  m and  $\theta = 0^\circ$ . SNR values between 15 and 65 dB have been realized by varying the amount of noise on the signal. Around 14 dB, the signal amplitude falls below the threshold, and therefore a TOF measurement cannot be obtained. In comparing the various methods, our purpose is to determine the method(s) which most consistently result in the best performance, over the range of  $r$ ,  $\theta$ , and SNR. This is because, even if we know the noise level, the signal level and thus the SNR will depend on  $r$  and  $\theta$ , which are the very quantities one is trying to determine with such systems in the first place.

We begin our comparison of the several methods by comparing the four variations of the sliding-window method among themselves. For all forms of the signal (i.e., O, R, or E), sliding-window (A), (C), (D) have equal standard deviations as expected. This is because, for a given window

**Table 1.** Simulation and experimental results for  $r = 0.5$  m,  $\theta = 0^\circ$ , and SNR = 35 dB. THD: thresholding, SW: sliding window, CUF: curve fitting, COR: correlation, O: original, R: rectified, E: envelope.

Method		Simulation (SNR = 35 dB)			Experiment (SNR = 35 dB)		
		$b$ (cm)	$\sigma$ (cm)	$\mathcal{E}$ (cm)	$b$ (cm)	$\sigma$ (cm)	$\mathcal{E}$ (cm)
THD	O	0.671	0.082 2	0.676	0.585	0.0793	0.590
	R	0.666	0.084 3	0.672	0.582	0.0790	0.587
	E	0.586	0.052 4	0.588	0.519	0.0681	0.523
SW(A)	O	-0.228	0.039 4	0.231	-0.229	0.0432	0.233
	R	-0.232	0.041 5	0.235	-0.227	0.0449	0.231
	E	-0.448	0.034 8	0.449	-0.423	0.0322	0.425
SW(B)	O	0.671	0.082 2	0.676	0.585	0.0793	0.590
	R	0.666	0.084 3	0.672	0.582	0.0790	0.587
	E	0.586	0.052 4	0.588	0.519	0.0681	0.523
SW(C)	O	0.459	0.039 4	0.461	0.460	0.0432	0.462
	R	0.455	0.041 5	0.457	0.458	0.0449	0.460
	E	0.239	0.034 8	0.241	0.225	0.0322	0.227
SW(D)	O	1.146	0.039 4	1.147	1.147	0.0432	1.148
	R	1.142	0.041 5	1.143	1.145	0.0449	1.146
	E	0.926	0.034 8	0.927	0.912	0.0322	0.913
CUF(A)	O	0.436	0.242	0.499	0.428	0.227	0.484
	R	-0.269	0.053 4	0.274	-0.216	0.0613	0.225
	E	-0.261	0.034 5	0.263	-0.227	0.0361	0.230
CUF(B)	O	-0.578	0.301	0.652	-0.515	0.290	0.591
	R	-0.507	0.309	0.594	-0.472	0.283	0.550
	E	-0.530	0.161	0.554	-0.502	0.142	0.522
COR	O	0.000	0.000 001 87	0.000 001 87	-0.000 344	0.0185	0.0185
	R	0.000	0.000 001 87	0.000 001 87	-0.004 47	0.0298	0.0301
	E	0.000	0.000 001 87	0.000 001 87	-0.005 23	0.0312	0.0316

length  $N$ , the points taken as TOF in these variations (the very first, central, and the  $(N - m)$ th samples of the window) remain fixed with respect to each other. Variation (B), on the other hand, exhibits a larger standard deviation than (A), (C), and (D). For larger values of  $r$  or  $|\theta|$ , or smaller values of SNR, we observe that variation (A) gives the smallest bias, followed by variations (B), (C), and (D) in the given order. Among the sliding-window variations, (B), (C) and (D) would never be used since (A) can offer the same standard deviation with smaller bias error than (C) and (D), and it can offer both smaller bias and smaller standard deviation than (B). Thus, sliding window (A) emerges as the method of choice for larger  $r$  or  $|\theta|$ , or smaller SNR. It is important to note that this conclusion follows regardless of the relative importance attached to minimizing bias and standard deviation. For smaller  $r$  or  $|\theta|$ , or larger SNR, however, the situation is more complicated and none of the variations is clearly superior to the others. For this method, we emphasize that it is immaterial whether we use O, R, or E since all give similar bias, standard deviation, and total error.

The bias errors of both sliding-window and thresholding methods increase with  $r$  and  $|\theta|$ . In contrast, the bias error of CUF(A) is relatively constant over the  $r$ ,  $\theta$  and SNR values considered, and is generally smaller. It is followed by CUF(B), and the other methods. (These biases for CUF(A) are obtained when the envelope of the signal is processed. Had the original or the rectified signal been used, the bias would have been worse due to the fluctuations of the waveform around the onset of the signal.)

On the other hand, the standard deviation of CUF(B) is the largest, followed by CUF(A) at SNRs below 20 dB, and

by thresholding and SW(B) at SNRs above 20 dB. Apart from the correlation method, smallest standard deviations are obtained with SW(A), (C), (D). Therefore, in terms of standard deviation, curve-fitting methods are not as good as the sliding window which offers the smallest standard deviation.

The total error turns out to be dominated by the bias and therefore has a shape which resembles the bias curve. In terms of bias and total error, CUF(A) shows the overall best performance. Although some of the variations of the sliding window result in smaller bias and total error over certain intervals, it would not be practical to exploit this since one does not know  $r$  and  $\theta$  to begin with. Thus, we conclude that CUF(A) is the method which most consistently results in lowest bias and total error over the range of parameters considered. On the other hand, in those instances where the standard deviation of the estimate is more important than the bias and total error, the method of choice would be sliding window, with the choice of variation as discussed previously.

In order of increasing computational complexity, the methods can be sorted as thresholding, sliding-window, curve fitting, and correlation detection. For the processing of a single echo, the required CPU times on a SUN SPARC 20 workstation are 5.6, 8.3 and 11.1 ms for the first three methods respectively. The classical correlation detection method would require many orders of magnitude greater time if the correlation method is performed at every possible sample shift: in other words if it is used as a detection method. In a practical implementation, the detection of the pulse could be performed by first thresholding and then applying the correlation only in the vicinity of the point where the

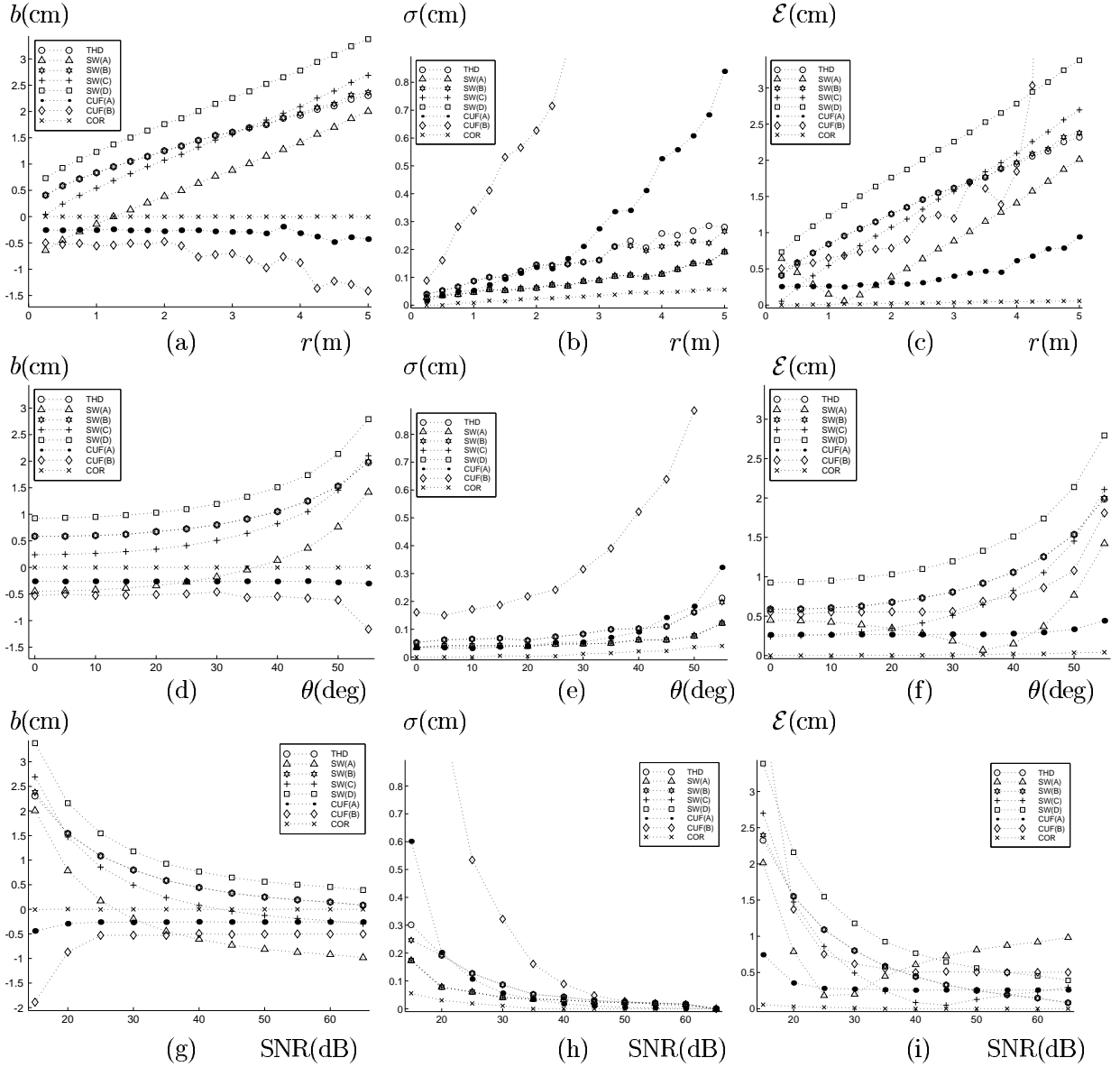


**Figure 2.** Variation of the bias, the standard deviation, and the total error of the TOF measurement with  $r$ ,  $\theta$ , and SNR when the signal envelope is used: (a) bias error versus range, (b) standard deviation versus range, (c) and total error versus range when  $\theta = 0^\circ$ ; (d) bias error versus azimuth, (e) standard deviation versus azimuth, (f) and total error versus azimuth when  $r = 0.5$  m; (g) bias error versus SNR, (h) standard deviation versus SNR, (i) and total error versus SNR when  $r = 0.5$  m and  $\theta = 0^\circ$ . THD: thresholding, SW: sliding window, CUF(A): least-squares curve fitting, CUF(B): analytical curve fitting, COR: correlation.

threshold was exceeded to get an accurate TOF measurement. Although such a hybrid thresholding/correlation method would be faster in a practical situation, it would still be difficult to implement, owing to the need to store many different templates which represent different points in the target position space.

#### 4. Experimental results

Experiments have been performed with Panasonic transducers, resonant at  $f_0 = 40$  kHz and exhibiting a relatively large half beamwidth of approximately  $60^\circ$  [18]. A planar target is positioned at  $r = 0.5$  m and  $\theta = 0^\circ$ . The block diagram of the ultrasonic measurement system is provided schematically

in figure 3. Data acquisition with this system is accomplished by using a PC A/D card with 12-bit resolution and 1 MHz maximum sampling frequency. In the current study, it was sufficient to sample the signals at 500 kHz. 5000 samples of each echo signal have been collected. A typical waveform obtained from the system is shown in figure 4. Echo signals are postprocessed on a SUN SPARC 20 workstation. An average over 100 noisy echo signals is computed to produce the correlation template for the original signal. Similarly, templates are generated for processing the rectified signal and the signal envelope. Experimentally obtained biases, standard deviations, and total errors for all four methods, computed over 100 echo waveforms, are tabulated in table 1. The results are in very good agreement with the corresponding simulation results.

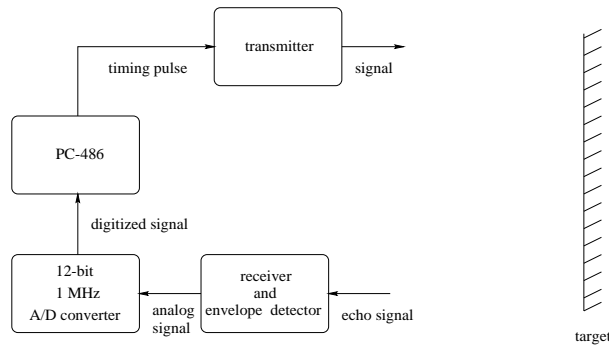


**Figure 3.** Block diagram of the data acquisition system and a target.

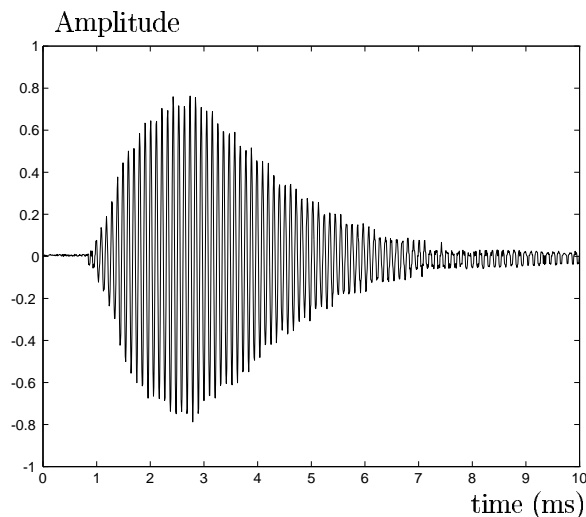


**Figure 4.** Typical echo waveform obtained from the ultrasonic system.

## 5. Conclusion

In this paper, four range measurement methods are compared on the basis of bias error, standard deviation, total error, robustness to noise, and difficulty/complexity of implementation. Correlation detection always gives the best results and forms a basis for comparison for the simpler and faster suboptimal methods. However, it is also computationally the most complex, with certain disadvantages in a real-time implementation. It has been included mainly as a reference in this study. Curve fitting, sliding window, and thresholding follow correlation detection in the order of decreasing complexity and can offer acceptable performance at much lower cost. Performances of all methods have been investigated as a function of target distance, azimuth and SNR. Two variations of curve fitting and four variations of the sliding window have been considered. Apart from correlation detection, lowest bias and total error is most consistently obtained with least-squares curve-fitting applied to the signal envelope. The bias problem of the simple thresholding method is more enhanced for the relatively long rise-time of the echoes produced by currently

available low-bandwidth ultrasonic transducers for operation in air. For larger bandwidth transducers, the signal rise-time would be much smaller, reducing the bias and possibly obviating the need to use curve-fitting methods. In those instances where minimizing the standard deviation of the measurement is more important than minimizing the bias and the total error, sliding window emerges as the method of choice. For all forms of the signal (i.e., original, rectified, envelope), sliding-window variations (A), (C), (D) have equal standard deviations. This value of the standard deviation is also the smallest among all the methods. Depending on the relative importance of bias and standard deviation for a given application, the method of choice can be determined. Since bias is the dominant component of the total error, developing algorithms that are robust to bias errors are of interest. The experimental results are in very good agreement with the corresponding simulation results. Overall, the three simple and fast processing methods provide a variety of attractive compromises between measurement accuracy and system complexity.

## Acknowledgments

This work was partially supported by TÜBİTAK under grant EEEAG-197E051. The author would like to thank Birsal Ayrulu for collecting the experimental data and the anonymous referee for invaluable comments and suggestions.

## References

- [1] Kleeman L and Kuc R 1995 *Int. J. Robot. Res.* **14** 295–318
- [2] Wazenski M and Alexandrou D 1997 *J. Acoust. Soc. Am.* **101** 1961–70
- [3] Bar-Shalom Y (ed) 1990 *Multitarget–Multisensor Tracking* (Norwood, MA: Artech House)
- [4] Canali C *et al* 1982 *IEEE Trans. Ind. Electron.* **29** 336–41
- [5] Cracknell A P 1982 *Ultrasonics* (London: Wykeham)
- [6] Barshan B 1991 A sonar-based mobile robot for bat-like prey capture *PhD Thesis* Yale University
- [7] Barshan B and Kuc R 1992 *IEEE Trans. Syst. Man Cybern.* **22** 636–46
- [8] McMullan W G, Delanghe B A and Bird J S 1996 *IEEE Trans. Instrum. Meas.* **45** 823–7
- [9] Press W H, Flannery B P, Teukolsky S A and Vetterling W T 1989 *Numerical Recipes in Pascal* (Cambridge: Cambridge University Press) pp 574–9
- [10] Barshan B and Ayrulu B 1998 *Electron. Lett.* **34** 1616–7
- [11] DiFranco J V and Rubin W L 1980 *Radar Detection* (Dedham, MA: Artech House)
- [12] Peremans H, Audenaert K and Van Campenhout J M 1993 *IEEE Trans. Robot. Autom.* **9** 36–48
- [13] Parrilla M, Anaya J J and Fritsch C 1991 *IEEE Trans. Instrum. Meas.* **40** 759–63
- [14] Papoulis A 1984 *Probability, Random Variables and Stochastic Processes* 2nd edn (New York: McGraw-Hill)
- [15] Freitag L E and Tyack P L 1993 *J. Acoust. Soc. Am.* **93** 2197–205
- [16] Zemanek J 1971 *J. Acoust. Soc. Am.* **49** 181–91
- [17] Bozma Ö I 1992 A physical model-based approach to analysis of environments using sonar *PhD Thesis* Yale University
- [18] Panasonic Corporation 1989 *Ultrasonic Ceramic Microphones* (Burlington, MA: Panasonic)